

Enhancing performance of inverted quantum-dot light-emitting diodes based on a solution-processed hole transport layer via ligand treatment

Depeng Li^{1,2}, Jingrui Ma^{1,2}, Wenbo Liu^{1,2}, Guohong Xiang^{1,2}, Xiangwei Qu^{1,2}, Siqi Jia^{3,†}, Mi Gu^{1,2}, Jiahao Wei^{1,2}, Pai Liu^{1,2}, Kai Wang^{1,2}, and Xiaowei Sun^{1,2,†}

¹Institute of Nanoscience and Applications, and Department of Electrical and Electronic Engineering, Southern University of Science and Technology, Shenzhen 518055, China

²Key Laboratory of Energy Conversion and Storage Technologies (Southern University of Science and Technology), Ministry of Education, Guangdong University Key Laboratory for Advanced Quantum Dot Displays and Lighting, and Shenzhen Key Laboratory for Advanced Quantum Dot Displays and Lighting, Southern University of Science and Technology, Shenzhen 518055, China

³Institute of Advanced Displays and Imaging, Henan Academy of Sciences, Zhengzhou 450046, China

Abstract: The performance of inverted quantum-dot light-emitting diodes (QLEDs) based on solution-processed hole transport layers (HTLs) has been limited by the solvent-induced damage to the quantum dot (QD) layer during the spin-coating of the HTL. The lack of compatibility between the HTL's solvent and the QD layer results in an uneven surface, which negatively impacts the overall device performance. In this work, we develop a novel method to solve this problem by modifying the QD film with 1,8-diaminooctane to improve the resistance of the QD layer for the HTL's solvent. The uniform QD layer leads the inverted red QLED device to achieve a low turn-on voltage of 1.8 V, a high maximum luminance of 105 500 cd/m², and a remarkable maximum external quantum efficiency of 13.34%. This approach releases the considerable potential of HTL materials selection and offers a promising avenue for the development of high-performance inverted QLEDs.

Key words: quantum dots; quantum-dot light-emitting diodes; inverted structure; ligand treatment

Citation: D P Li, J R Ma, W B Liu, G H Xiang, X W Qu, S Q Jia, M Gu, J H Wei, P Liu, K Wang, and X W Sun, Enhancing performance of inverted quantum-dot light-emitting diodes based on a solution-processed hole transport layer via ligand treatment[J]. *J. Semicond.*, 2023, 44(9), 092603. <https://doi.org/10.1088/1674-4926/44/9/092603>

1. Introduction

Colloidal quantum dots (QDs) have garnered significant interest in next-generation displays and lighting^[1–3] owing to their outstanding advantages, such as narrow emission linewidth^[4, 5], size tunable emission wavelength^[6, 7] and low-cost solution processing^[8–12]. In the past few decades, the performance of quantum-dot light-emitting diodes (QLEDs) has been significantly improved through various means including the improvement of material synthesis^[13–15] and device structure design^[16–18]. To date, the external quantum efficiency (EQE) of red, green, and blue QLED devices has been significantly improved, with values of 33.1%^[19], 28.7%, and 21.9%^[20], respectively. Moreover, the lifetime of red and green QLEDs have met the standard for the display industry^[21–23].

Nowadays, two conventional architectures are employed for QLED devices, the normal structure and the inverted structure. The normal QLED is structured as a substrate/anode/hole injection layer (HIL)/hole transport layer (HTL)/QDs/electron transport layer (ETL)/cathode, while the inverted QLED comprises substrate/cathode/ETL/QDs/HTL/HIL/anode^[23, 24].

Many published works have been centered on normal QLEDs^[13, 19, 20, 25–27] and the champion QLEDs adopted the normal structure. Meanwhile, all QLEDs with long lifetime regard the Poly[(9,9-dioctylfluorenyl-2,7-diyl)-co-(4,4'-(N-(4-sec-butylphenyl)diphenylamine))] (TFB) or its derivant as HTL material^[20, 22, 26, 28]. However, the normal architecture presents challenges in integration with low-cost n-type metal oxide or amorphous silicon-based thin-film transistors (TFTs). The direct connection between the cathode of inverted QLEDs and the drain of TFTs makes the inverted structure a better choice for the display industry^[1, 16]. In addition, TFB is incompatible in inverted devices directly, because when the TFB spins on the QD layer, the non-orthogonal solvent will severely erode the QD layer, resulting in a dramatic reduction in device performance.

To prevent the QD EML from being disrupted when fabricating the HTL, several strategies have been implemented. Liu *et al.* dissolved the HTL in orthogonal solvents such as 1,4-dioxane^[1]. However, most of the device performances are unideal and TFB exhibits poor solubility in this solvent. Some groups reported the addition of a protective layer such as polyethylenimine ethoxylated (PEIE) between the QD EML and HTL to protect the QD layer^[29, 30]. In addition, some ligands and cross-linkers, such as hexamethyldisilazane (HMDS) and 6-mercaptohexanol, are used to modify the surface of the QD film^[31, 32]. However, the interlayer and cross-linkers materials used are typically electrically insulating to impede

Correspondence to: S Q Jia, jasiqi12@163.com; X W Sun, sunxw@sustech.edu.cn

Received 21 MAY 2023; Revised 5 JULY 2023.

©2023 Chinese Institute of Electronics

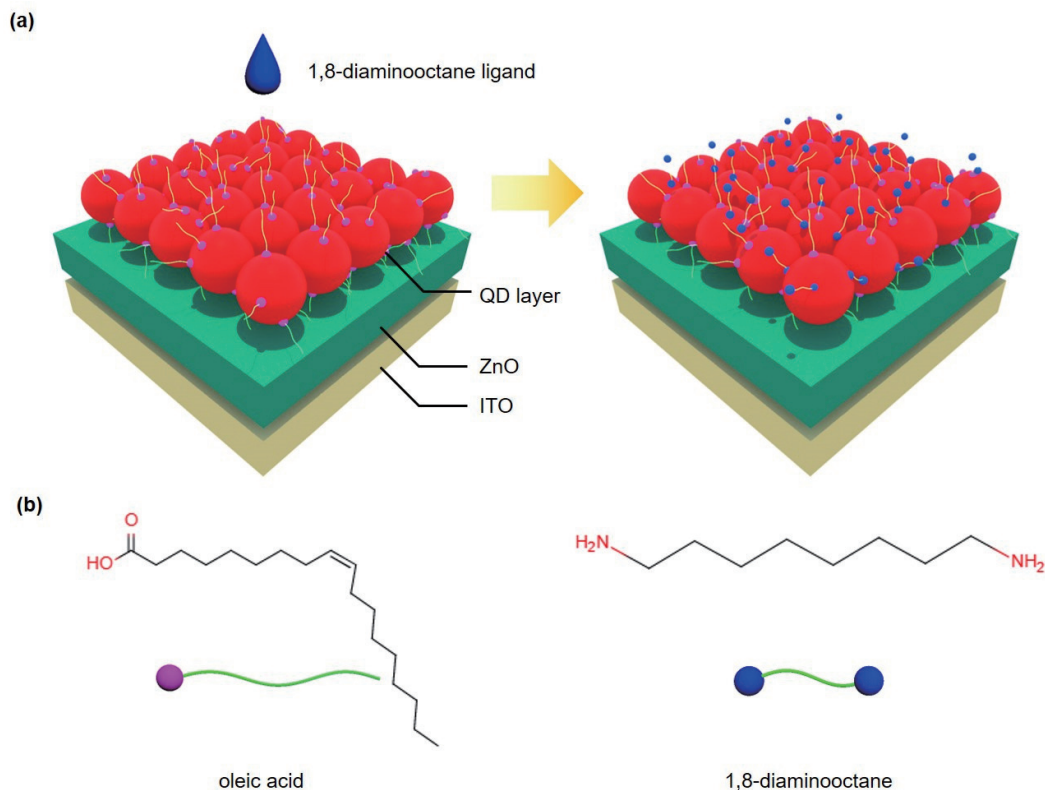


Fig. 1. (Color online) (a) Schematic illustration of the 1,8-diaminooctane ligand treatment process, (b) chemical structure (top) and graphical sketch (bottom) of the oleic acid and 1,8-diaminooctane ligand. The purple and blue balls represent the carboxyl and amine groups, respectively, and the green line is the carbon chain.

the carrier injection, thereby limiting the performance of QLEDs.

In order to achieve inverted QLEDs based on TFB with high performance, it is crucial to enhance the QD layer's resistance against TFB solvent, chlorobenzene (CB). In our study, a facile solid-film ligand treatment approach was employed to modify the surface of QD films, resulting in the enhanced resistance of the QD films to non-polar solvents such as CB. After ligand treatment, a uniform and smooth TFB film was formed on the undamaged QD layer. Remarkably, the inverted red QLED device with a low turn-on voltage of 1.8 V, a maximum luminance of 105 500 cd/m^2 , and a maximum EQE of 13.34% was achieved. These results represent significant improvements over untreated QLED devices, thereby underscoring the potential of this work to promote further research interest in developing practical applications for QLEDs.

2. Result and discussion

Inspired by bifunctional ligands during the deposition of multiple QD layers^[33–35], we developed a simple solid-film ligand treatment method in the process of inverted QLEDs. As shown in Fig. 1(a), the QD layers are treated by 1,8-diaminooctane ligands via spin-coating. This ligand acts as a cross-linking molecule thanks to the amino functional groups at both ends of the octane alkyl chain^[33]. It adsorbs onto the QD surface and forms strong anchors among QDs^[36] (Fig. 1(b)). Additionally, the partial substitution of long-chain ligands such as oleic acid with short-chain ligands can enhance the charge transport capability^[37, 38].

The UV-vis absorption spectra show that the first exciton absorption peaks at around 617 nm (Fig. 2(a)), indicating that

this treatment has little impact on the energy gap of the QD layer. Fig. 2(b) demonstrates that the photoluminescence (PL) intensity of the QD layer after ligand treatment is slightly lower than that of the untreated QD layer. Additionally, the photoluminescence quantum yield (PLQY), PL peak, and full width at half maximum (FWHM) of the QD film are similar, as shown in Table S1. These results suggest the ligand treatment will not lead to a decrease in the PL performance of the QD layer, which is the premise for realizing high performance devices. The PL image of QD films before and after ligand treatment, as illustrated in the inset of Fig. 2(b), reveals that the ligand treatment shows no damage to the evenness of QD layer. Time-resolved PL results of QD films are shown in Fig. 2(c). The PL decay of the QD films before and after treatment is essentially the same, which suggests that this method does not cause additional surface traps to QDs. These results indicate that the ligand treatment does not significantly damage the QD layer and retains its excellent luminescent properties. As for the resistance to the solvent CB, shown in Fig. 2(d), the ligand-treated QD film can withstand rinsing with CB, and the PL intensity is mostly retained compared to the untreated QD film. These observations suggest that the incorporation of 1,8-diaminooctane does not significantly damage the QD layer, but improves its tolerance to CB.

To illustrate the impact of ligand treatment and CB rinsing on the film morphology, SEM and AFM measurement were conducted, as shown in Fig. 3 and Fig. S1. The pristine QD film shows the smooth and dense surface with low roughness of 1.87 nm (Figs. 3(a) and 3(c)). As expected, after rinsing with CB, the film becomes discontinuous, and some noticeable voids appear on the surface due to the dissolution of CB

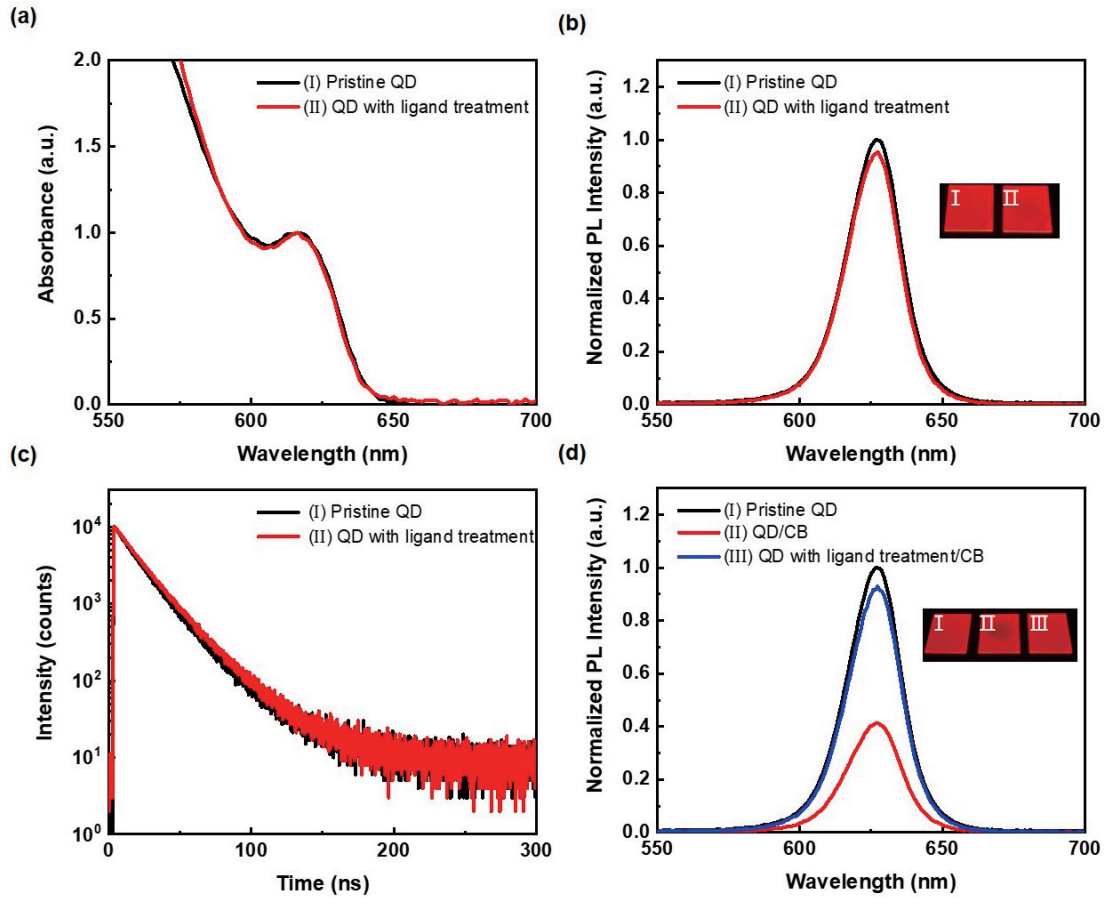


Fig. 2. (Color online) Characterization of the QD films. (a) UV-vis absorption spectra, (b) PL spectra and (c) time-resolved PL decay of the QD films before and after ligand treatment. The inset of (b): the corresponding PL image of the QD films under 365 nm LED excitation. (d) The PL spectra of the pristine and ligand-treated QD films rinsed with CB. The inset of (d): PL image (under 365 nm) of corresponding PL image of the QD films.

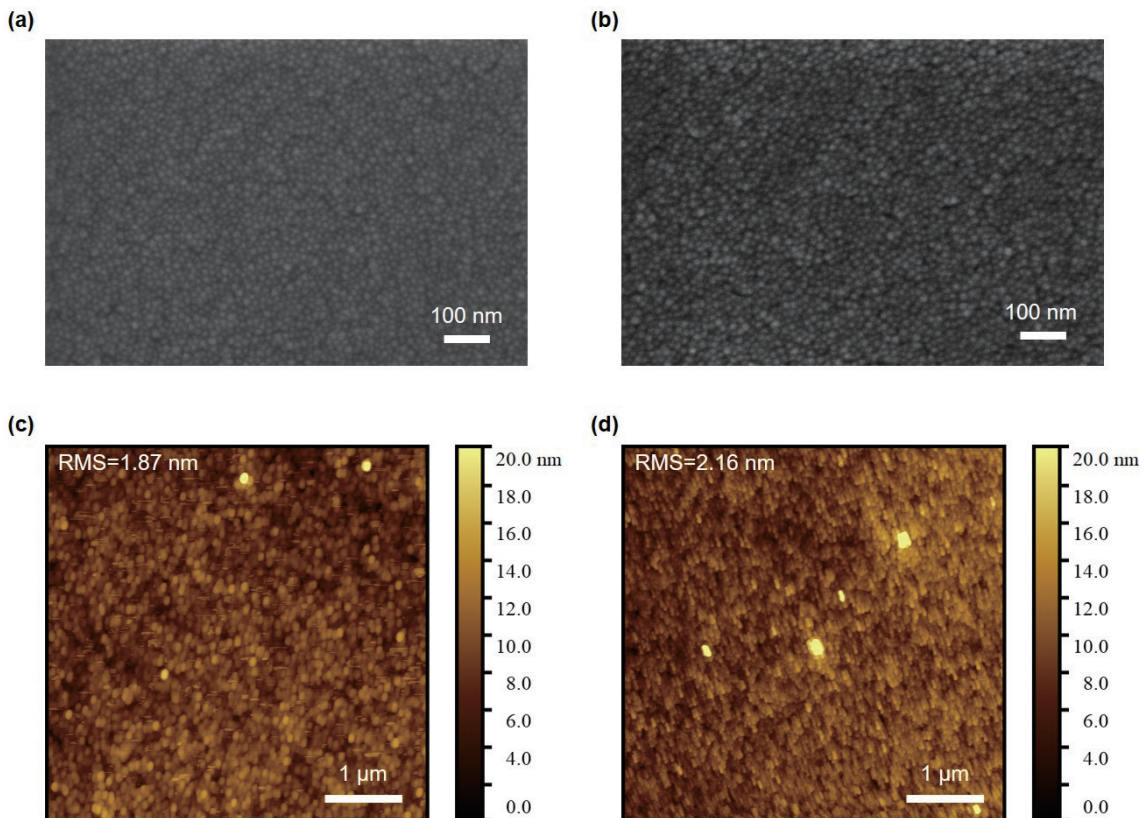


Fig. 3. (Color online) SEM images of the (a) pristine QD film and (b) ligand-treated QD film. AFM images of the (c) pristine QD film and (d) ligand-treated QD film.

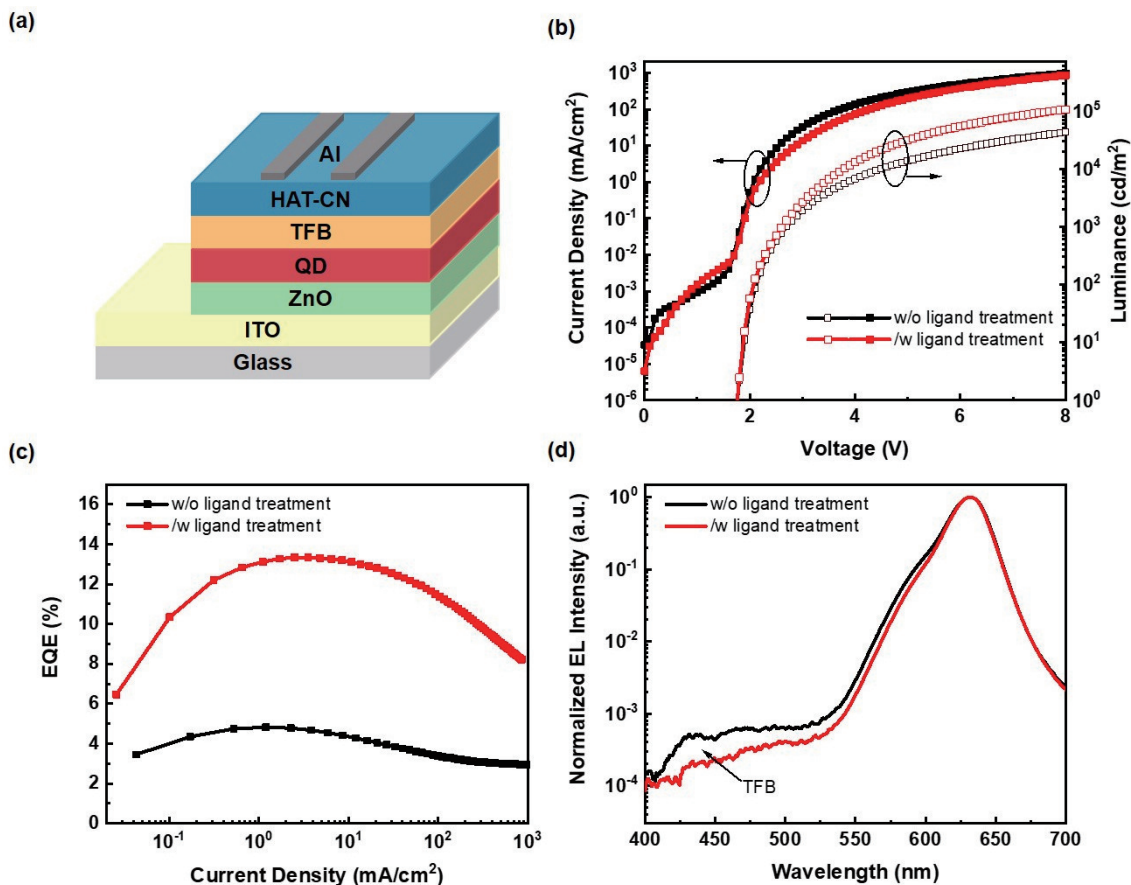


Fig. 4. (Color online) Device characteristics of inverted QLED. (a) Device structure, (b) J - V - L characteristics, (c) EQE- J characteristics, and (d) EL spectra of the inverted device (at 8 V).

Table 1. The device characteristics of inverted QLEDs.

Method	V_{on} (V) (at 1 cd/m ²)	V_{driving} (V) (at 100 cd/m ²)	EQE (%)		L_{max} (cd/m ²)
			100/1000/10 000 cd/m ²	Max	
w/o ligand treatment	1.8	2.1	4.83/4.16/3.15	4.83	42 980
/w ligand treatment	1.8	2.2	12.84/13.31/12.04	13.34	105 500

to the QD layer (Fig. S1(a)). The AFM image reveals the presence of distinct bumps, which further suggests that the rinsing of CB inflicts serious damage to the QD layer (Fig. S1(c)). In contrast, after the ligand treatment, the film surface has no significant voids and exhibits a similar roughness and density as the pristine film (Figs. 3(b) and 3(d)). The improved resistance of the QD film with ligand treatment to CB is further confirmed by the surface morphology (Figs. S1(b) and (d)). The roughness of the ligand-treated QD film has increased compared to the pristine QD film, but the surface remains dense, and the size of the cracks and voids is smaller than that of the pristine QD rinsed with CB. These results indicate the protective role of ligand treatment on QD film during device fabrication.

To demonstrate the effect of ligand treatment on the performance of inverted QLED, two types of QLEDs, with and without ligand treatment, were fabricated. The architecture of the inverted QLED is illustrated in Fig. 4(a). The device consists of stacked layers of ITO/ZnO/QD/TFB/HAT-CN/Al. The ZnO is used as the ETL. TFB and HAT-CN are the HTL and HIL, respectively. The current density-luminance-voltage (J - V - L) and EQE- J curves for the two devices are shown in Figs. 4(b) and

4(c), respectively. Remarkably, the device with ligand treatment demonstrates a significantly improved performance, as indicated by the data summarized in Table 1. As shown in Fig. 4(b), the leakage current of the untreated device is larger than the ligand-treated device, which can be attributed to the increased electron leakage channels induced by the uneven surface of the QD film (Fig. S1(a)). The turn-on voltage of the ligand-treated device is similar to that of the untreated device, at 1.8 V, which indicates that the ligand treatment does not hinder carrier injection. The ligand-treated device achieves a much higher brightness of 105 500 cd/m² at 8 V compared to the untreated device's 42 980 cd/m². Additionally, the EQE is increased by a factor of 2.76 after ligand treatment, reaching a maximum value of 13.34%. The above results suggest the ligands treatment approach is highly effective for fabricating inverted QLEDs based on solution-processed HTL. The electroluminescence (EL) spectra of two QLEDs under 8 V are presented in Fig. 4(d). Both the EL emissions are centered at 630 nm with a narrow FWHM of 27 nm. However, the parasitic emission from the TFB (blue region, EL emission spectrum of TFB is shown in Fig. S2) is observed in the EL spectrum of the device without ligand treatment

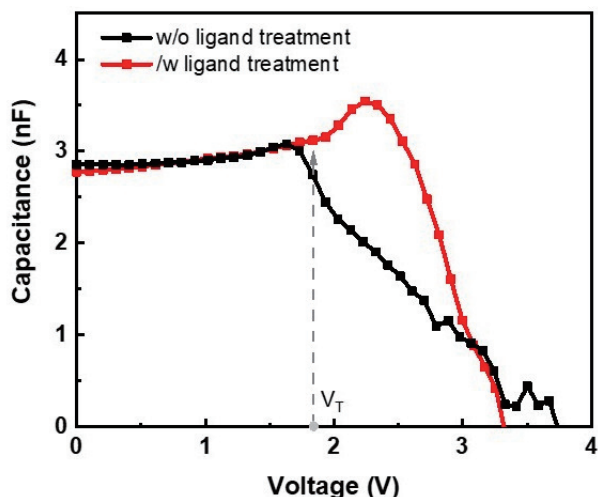


Fig. 5. (Color online) Capacitance–voltage characteristics of the inverted devices, $f = 1$ kHz.

(Fig. 4(d) (arrows)). Thus, these results also indicate that the untreated QD film is severely dissolved and eroded during the HTL layer deposition, leading to excessive electron leakage into the HTL layer and causing a further reduction in device efficiency and performance^[20]. The ligand treatment, which reduces the damage to the QD from CB and the electron leakage problem, offers an effective solution for fabricating inverted QLEDs.

The operational stability of QLEDs is also significantly improved by the implementation of ligand treatment. At an initial luminance of 1000 cd/m^2 , the ligand-treated device has an operational lifetime T_{50} of 583 hours greater than the untreated device ($T_{50} = 442 \text{ h}$) (Fig. S3). By applying the equation $L_0^n T_{50} = \text{constant}$ ^[39] (L_0 and n are the initial luminance and acceleration factor) with $n = 1.8$ ^[40–42], the T_{50} lifetime for the ligand-treated device is estimated to be 36 785 h at 100 cd/m^2 , whereas the T_{50} lifetime for the untreated device is estimated to be only 27 888 h.

The capacitance–voltage (C – V) provides valuable insights into carrier dynamics in QLEDs^[35, 43–46]. The C – V characteristics of both the untreated and ligand-treated devices are shown in Fig. 5 at the frequency of 1 kHz. The device capacitance is predominantly governed by the geometrical capacitance at 0 V. The ligand-untreated device has a slightly higher geometrical capacitance (2.86 nF) compared to the treated device (2.78 nF). Statistical analysis of geometrical capacitance exhibits similar results (Fig. S4) across different frequencies. The higher geometrical capacitance of untreated devices may be due to the thinning of the QD layer during the TFB spin-coating. As the voltage increases, electrons gradually inject and accumulate in the device, resulting in capacitance rise^[43]. For the ligand-treated device, there is a capacitance peak (3.54 nF) at 2.2 V due to the electron accumulation at the QD/HTL interface^[47, 48]. Afterward, the capacitance drops sharply, which is attributed to the effective recombination of electrons and holes. However, for the untreated device, the capacitance begins to drop at 1.6 V and does not exhibit an obvious peak. This indicates a low level of charge accumulation in the untreated device, since numerous leakage paths are formed during the TFB fabrication, as observed by the morphology results shown in Fig. S1.

3. Conclusion

In conclusion, this study developed a ligand-treatment approach on QD films to prevent damage to the QD layer during TFB layer deposition. After the treatment of QD film with a 1,8-diaminooctane ligand, the inverted QLED possesses higher efficiency, higher brightness, and longer operational lifetime than the untreated QLED. These findings firmly indicate that the treatment of QD film with ligands is a simple and effective strategy for fabricating high-performance inverted QLED. We expect this study to provide a feasible solution for inverted QLED.

Acknowledgments

This work was supported by the National Key Research and Development Program of China (Nos. 2021YFB3602703, 2022YFB3606504, and 2022YFB3602903), National Natural Science Foundation of China (No. 62122034), Guangdong University Key Laboratory for Advanced Quantum Dot Displays and Lighting (No. 2017KSYS007), and Shenzhen Key Laboratory for Advanced Quantum Dot Displays and Lighting (No. ZDSYS201707281632549), Shenzhen Science and Technology Program (No. JCYJ20220818100411025), and Shenzhen Development and Reform Commission Project (No. XMHT20220114005).

Appendix A. Supplementary materials

Supplementary materials to this article can be found online at <https://doi.org/1674-4926/44/9/092603>.

References

- [1] Liu Y, Jiang C B, Song C, et al. Highly efficient all-solution processed inverted quantum dots based light emitting diodes. *ACS Nano*, 2018, 12, 1564
- [2] Kim T H, Cho K S, Lee E K, et al. Full-colour quantum dot displays fabricated by transfer printing. *Nature Photon*, 2011, 5, 176
- [3] Hong A, Kim J, Kwak J. Sunlike white quantum dot light-emitting diodes with high color rendition quality. *Adv Optical Mater*, 2020, 8, 2001051
- [4] Bae W K, Lim J, Lee D G, et al. R/G/B/natural white light thin colloidal quantum dot-based light-emitting devices. *Adv Mater*, 2014, 26, 6387
- [5] Lim J, Park Y S, Wu K F, et al. Droop-free colloidal quantum dot light-emitting diodes. *Nano Lett*, 2018, 18, 6645
- [6] Peng Z A, Peng X G. Formation of high-quality CdTe, CdSe, and CdS nanocrystals using CdO as precursor. *J Am Chem Soc*, 2001, 123, 183
- [7] Murray C B, Norris D J, Bawendi M G. Synthesis and characterization of nearly monodisperse CdE (E = sulfur, selenium, tellurium) semiconductor nanocrystallites. *J Am Chem Soc*, 1993, 115, 8706
- [8] Colvin V L, Schlamp M C, Alivisatos A P. Light-emitting diodes made from cadmium selenide nanocrystals and a semiconducting polymer. *Nature*, 1994, 370, 354
- [9] Liu M X, Yazdani N, Yarema M, et al. Colloidal quantum dot electronics. *Nat Electron*, 2021, 4, 548
- [10] Meng T T, Zheng Y T, Zhao D L, et al. Ultrahigh-resolution quantum-dot light-emitting diodes. *Nat Photon*, 2022, 16, 297
- [11] Jia S Q, Tang H D, Ma J R, et al. High performance inkjet-printed quantum-dot light-emitting diodes with high operational stability. *Adv Opt Mater*, 2021, 9, 2101069
- [12] Zhao J Y, Chen L X, Li D Z, et al. Large-area patterning of full-colour quantum dot arrays beyond 1000 pixels per inch by selective electrophoretic deposition. *Nat Commun*, 2021, 12, 4603

- [13] Yang Y X, Zheng Y, Cao W R, et al. High-efficiency light-emitting devices based on quantum dots with tailored nanostructures. *Nature Photon*, 2015, 9, 259
- [14] Shen H B, Cao W R, Shewmon N T, et al. High-efficiency, low turn-on voltage blue-violet quantum-dot-based light-emitting diodes. *Nano Lett*, 2015, 15, 1211
- [15] Duan X J, Ma J R, Zhang W D, et al. Study of the interfacial oxidation of InP quantum dots synthesized from tris(dimethylamino) phosphine. *ACS Appl Mater Interfaces*, 2023, 15, 1619
- [16] Kwak J, Bae W K, Lee D G, et al. Bright and efficient full-color colloidal quantum dot light-emitting diodes using an inverted device structure. *Nano Lett*, 2012, 12, 2362
- [17] Zhang H, Chen S M, Sun X W. Efficient red/green/blue tandem quantum-dot light-emitting diodes with external quantum efficiency exceeding 21%. *ACS Nano*, 2018, 12, 697
- [18] Mei G D, Wang W G, Wu D, et al. Full-color quantum dot light-emitting diodes based on microcavities. *IEEE Photonics J*, 2022, 14, 1
- [19] Wang L S, Lin J, Lv Y, et al. Red, green, and blue microcavity quantum dot light-emitting devices with narrow line widths. *ACS Appl Nano Mater*, 2020, 3, 5301
- [20] Deng Y Z, Peng F, Lu Y, et al. Solution-processed green and blue quantum-dot light-emitting diodes with eliminated charge leakage. *Nat Photon*, 2022, 16, 505
- [21] Liu D Q, Cao S, Wang S Y, et al. Highly stable red quantum dot light-emitting diodes with long T_{95} operation lifetimes. *J Phys Chem Lett*, 2020, 11, 3111
- [22] Li X Y, Lin Q L, Song J J, et al. Quantum-dot light-emitting diodes for outdoor displays with high stability at high brightness. *Adv Optical Mater*, 2020, 8, 1901145
- [23] Kim J, Roh J, Park M, et al. Recent advances and challenges of colloidal quantum dot light-emitting diodes for display applications. *Adv Mater*, 2023, 2212220
- [24] Hu Q Q, Si J J, Chen D S, et al. High-performance all-solution-processed inverted quantum dot light-emitting diodes enabled by water treatment. *Nano Res*, 2023, 16, 10215
- [25] Dai X L, Zhang Z X, Jin Y Z, et al. Solution-processed, high-performance light-emitting diodes based on quantum dots. *Nature*, 2014, 515, 96
- [26] Cao W R, Xiang C Y, Yang Y X, et al. Highly stable QLEDs with improved hole injection via quantum dot structure tailoring. *Nat Commun*, 2018, 9, 2608
- [27] Won Y H, Cho O, Kim T, et al. Highly efficient and stable InP/ZnSe/ZnS quantum dot light-emitting diodes. *Nature*, 2019, 575, 634
- [28] Chen X T, Lin X F, Zhou L K, et al. Blue light-emitting diodes based on colloidal quantum dots with reduced surface-bulk coupling. *Nat Commun*, 2023, 14, 284
- [29] Kim D, Fu Y, Kim S, et al. Polyethylenimine ethoxylated-mediated all-solution-processed high-performance flexible inverted quantum dot-light-emitting device. *ACS Nano*, 2017, 11, 1982
- [30] Lee W, Kim B, Choi Y, et al. Polyethylenimine-ethoxylated dual interfacial layers for highly efficient and all-solution-processed inverted quantum dot light-emitting diodes. *Opt Express*, 2020, 28, 33971
- [31] Fu Y, Kim D, Moon H, et al. Hexamethyldisilazane-mediated, full-solution-processed inverted quantum dot-light-emitting diodes. *J Mater Chem C*, 2017, 5, 522
- [32] Lee W, Lee C M, Kim B, et al. Enhancing the efficiency of solution-processed inverted quantum dot light-emitting diodes via ligand modification with 6-mercaptophexanol. *Opt Lett*, 2021, 46, 1434
- [33] Kozlov O V, Park Y S, Roh J, et al. Sub-single-exciton lasing using charged quantum dots coupled to a distributed feedback cavity. *Science*, 2019, 365, 672
- [34] Roh J, Park Y S, Lim J, et al. Optically pumped colloidal-quantum-dot lasing in LED-like devices with an integrated optical cavity. *Nat Commun*, 2020, 11, 271
- [35] Qu X W, Xiang G H, Ma J R, et al. Identifying the dominant carrier of CdSe-based blue quantum dot light-emitting diode. *Appl Phys Lett*, 2023, 122, 113501
- [36] Rhee S, Jeong B G, Choi M, et al. Versatile use of 1, 12-diaminododecane as an efficient charge balancer for high-performance quantum-dot light-emitting diodes. *ACS Photonics*, 2023, 10, 500
- [37] Lee S, Choi M J, Sharma G, et al. Orthogonal colloidal quantum dot inks enable efficient multilayer optoelectronic devices. *Nat Commun*, 2020, 11, 4814
- [38] Pu C D, Dai X L, Shu Y F, et al. Electrochemically-stable ligands bridge the photoluminescence-electroluminescence gap of quantum dots. *Nat Commun*, 2020, 11, 937
- [39] Scholz S, Kondakov D, Lüssem B, et al. Degradation mechanisms and reactions in organic light-emitting devices. *Chem Rev*, 2015, 115, 8449
- [40] Mude N N, Kim S J, Lampande R, et al. An efficient organic and inorganic hybrid interlayer for high performance inverted red cadmium-free quantum dot light-emitting diodes. *Nanoscale Adv*, 2022, 4, 904
- [41] Ye Y X, Zheng X R, Chen D S, et al. Design of the hole-injection/hole-transport interfaces for stable quantum-dot light-emitting diodes. *J Phys Chem Lett*, 2020, 11, 4649
- [42] Davidson-Hall T, Aziz H. Perspective: Toward highly stable electroluminescent quantum dot light-emitting devices in the visible range. *Appl Phys Lett*, 2020, 116, 010502
- [43] Ma J R, Tang H D, Qu X W, et al. A dC/dV measurement for quantum-dot light-emitting diodes. *Chin Phys Lett*, 2022, 39, 128401
- [44] Xiao X T, Ye T K, Sun J Y, et al. Capacitance-voltage characteristics of perovskite light-emitting diodes: Modeling and implementing on the analysis of carrier behaviors. *Appl Phys Lett*, 2022, 120, 243501
- [45] Zhang X W, Xu J W, Xu H R, et al. Elucidation of carrier injection and recombination characteristics with impedance and capacitance in organic light-emitting diodes and the frequency effects. *J Phys D: Appl Phys*, 2013, 46, 055102
- [46] Qu X W, Ma J R, Shan C W, et al. Trap state-assisted electron injection in blue quantum dot light-emitting diode. *Appl Phys Lett*, 2022, 121, 113507
- [47] Chung D S, Davidson-Hall T, Cotella G, et al. Significant lifetime enhancement in QLEDs by reducing interfacial charge accumulation via fluorine incorporation in the ZnO electron transport layer. *Nano Micro Lett*, 2022, 14, 1
- [48] Yuan Y, Xue X L, Wang T, et al. Polyethylenimine modified Sol-gel ZnO electron-transporting layers for quantum-dot light-emitting diodes. *Org Electron*, 2022, 100, 106393



Depeng Li received his B.E. degree in Electrical and Electronic Engineering from Southern University of Science and Technology in 2019, Guangdong, China. He is studying a Ph.D. degree in Southern University of Science and Technology currently. His research focuses on Micro-QLED and QLEDs device fabrication.



Siqi Jia received his doctoral degree from Jilin University, Changchun, China, in 2022. He is currently a Distinguished Research Fellow at Institute of Advanced Displays and Imaging, Henan Academy of Sciences. His current research interests include inkjet printing technology, optoelectronic materials and device.



Xiaowei Sun is a Chair Professor and the Executive Dean of the Institute of Nanoscience and Applications in the Southern University of Science and Technology, Shenzhen, China. He is an academican of the Asia-Pacific Academy of Materials, and the fellow of several other academic societies including Optica (formerly OSA), SPIE, and the Institute of Physics (UK). His main research presently is on high-quality displays based on nanocrystals and naked-eye 3D displays.